DIAPIR-INDUCED REORIENTATION OF ENCELADUS. Robert T. Pappalardo[1] and Francis Nimmo[2] [1]Laboratory for Atmospheric and Space Physics, University of Colorado, Boulder, CO 80309-0392; [2]Dept. Earth Sciences, University of California Santa Cruz, 1156 High St., Santa Cruz, CA 95064.

Introduction: The south polar region of Enceladus, a small icy satellite of Saturn, consists of young, tectonically deformed terrain and has an anomalously high heat flux [1,2]. We find that the pole-centered location of this region can be explained by reorientation of Enceladus induced by a large, low-density ice diapir within a relatively thick ice mantle. Poleward reorientation requires that Enceladus have a near-surface elastic ice layer in excess of ~1 km thickness.

Reorientation of Enceladus: We consider the circumstances under which a large, low-density diapir could have caused reorientation of Enceladus to move the diapiric region towards the satellite's maximum intertia (spin) axis. We model a large-scale low-density region embedded within an ice mantle and beneath an ice lithosphere (Fig. 1). If the overlying lithosphere has negligible rigidity, the mass deficit at depth will be compensated by a surface mass excess, generated by upwarped topography. Because that mass excess is closer to the surface than the interior mass deficit, the net effect is to generate a positive geoid anomaly, which would tend to reorient the region toward the equator. In contrast, for the case of an infinitely rigid lithosphere, there would be no surface topography, thus producing a net negative geoid anomaly, tending to reorient the region toward the pole. A subsurface diapir therefore can result in either poleward or equatorward reorientation, depending on the rigidity (or elastic thickness) of the lithosphere [3]. Reorientation is opposed by the frozen-in component of the triaxial satellite's tidal and rotational bulges [4,5]; thus, a satellite with lower rigidity will have smaller permanent bulges and is more likely to undergo reorientation.

The viscous relaxation timescale for a conductive ice layer is typically less than 1 Myr [6], so density anomalies which persist for periods long compared to this timescale are likely to lead to reorientation [5,7]. Following the approach of Matsuyama et al. [5], we find for a synchronously rotating satellite the angular reorientation δ due to an imposed geoid anomaly is

$$\delta = \frac{1}{2}\tan^{-1}\left(\frac{Q\beta\sin 2\theta_L}{n - Q\beta\cos 2\theta_L}\right) \qquad (1)$$

where θ_L is the initial colatitude of the geoid anomaly center, n is a parameter that varies from 1 to 4 depending on the longitude of the anomaly relative to the tidal bulge, Q parameterizes the size of the geoid anomaly, and β quantifies the non-hydrostatic component of rotational flattening, which opposes reorientation.

The quantity β is given by $\beta^{-1}=1-(k_f^T/k_f^{T*})$, where k_f^T and k_f^{T*} are the degree-two tidal Love numbers for the case when the lithosphere has finite and zero rigidity, respectively [5]. Larger β values indicate a situation closer to the zero-rigidity (fluid) case, resulting in a smaller permanent bulge and greater reorientation. Ross and Schubert [8] demonstrated that for a homogeneous Enceladus with a viscosity appropriate to that of ice near its melting temperature, k_f^T reaches values approaching 2/3 k_f^{T*}, giving $\beta \approx 3$. The presence of a rigid ice lithosphere will reduce this value; for example, using the two-layer analytical approach of [9], an elastic layer 4 km thick overlying a fluid interior gives β =1.2. This situation is appropriate to the case when a subsurface ocean decouples the ice mantle from the silicate core. Conversely, if the ice is directly coupled to the underlying silicates, the tidal deformation will be greatly reduced [10] and $(\beta - 1) \sim 10^{-4}$.

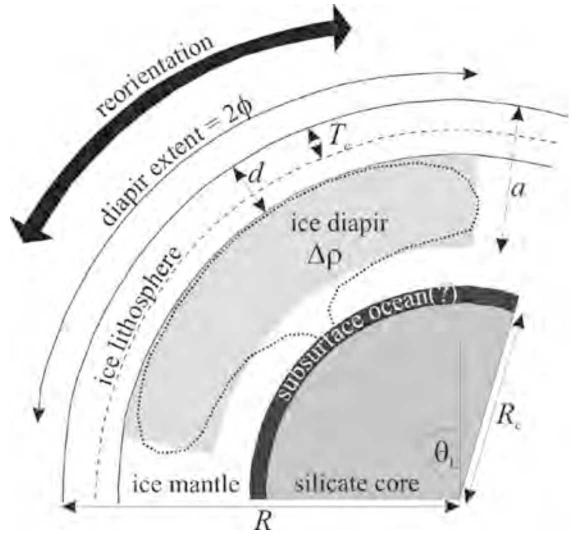

Fig. 1. Schematic diagram of a sub-surface diapir in a thick ice mantle on Enceladus. The light shaded area approximates the inferred diapir (dotted line) and has a density contrast $\Delta\rho$ with the surrounding ice. For ice and silicate densities of 950 kg m^{-3} and 3500 kg m^{-3}, respectively, R_c = 160 km using a bulk density for Enceladus of 1610 kg m^{-3}. We use a = 90 km, $\phi = 35^o$ and assume the initial load colatitude $\theta_L = 45^o$.

The second-degree geoid anomaly due to a partially compensated load of angular half-width ϕ and radial extent a-d (Fig. 1) is given to first order by

$$G_{20} = \pi G\left[\frac{R_C}{R}\right]^3 R_C(a-d)\Delta\rho\cos\phi\sin^2\phi \cdot\left(\left[C-1\right]+\left[2-C\right]\cdot\frac{a+d}{R_C}\right), \qquad (2)$$

where G is the gravitational constant, R is the mean satellite radius, R_C is the radius of the silicate core (for a diapir in the silicate core) or the radius of the satellite (for a diapir in the ice mantle), $\Delta\rho$ is the density contrast between the diapir and the surrounding material, and C is the degree of compensation ($0 < C < 1$). In the isostatic case $C = 1$ and the geoid anomaly is positive, as expected. The degree of compensation depends on the ability of the cold elastic part of the ice shell (T_e of Fig. 1) to resist deformation, and is calculated using the method of [11]. For a diapir within the ice shell, $R = R_C$; if a diapir occurs within the silicate core [12], the geoid anomaly is reduced by the factor $(R_C / R)^3$.

Fig. 2 shows the angular reorientation expected due to a diapir of $\phi = 35°$ emplaced at $\theta_L = 45^o$ as a function of lithospheric thickness d, where elastic thickness T_e = 0.4 d [13]. As expected, larger density contrasts lead to greater reorientation; low values of d lead to equatorward motion, while d > 2 km leads to poleward reorientation. The solid lines show the results using a β-value calculated using the methods described in [9]; the dashed lines assume that $\beta = 3$ [5] and demonstrate that larger reorientations occur if the permanent component of the tidal and rotational bulges is smaller. However, if the ice mantle is coupled to the silicate core, the reorientation is reduced (dotted line).

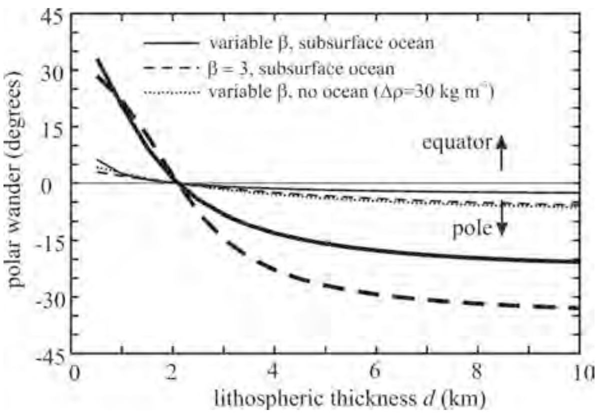

Fig. 2. Reorientation angle δ as a function of lithospheric thickness d calculated using eqn (1). Positive values of δ indicate equatorward reorientation; negative values indicate poleward reorientation. We use $\theta_L = 45^o$, $\phi = 35^o$, a = 90 km, n = 1, rigidity μ = 3 GPa; other parameters are defined in the caption to Fig. 1. Dashed curves assume $\beta = 3$ appropriate to a low-viscosity satellite, with density contrast $\Delta\rho$ = 10 kg m^{-3} (thin line) and 100 kg m^{-3} (thick line). Solid curves use these density contrasts but calculate β as a function of d, using the two-layer analytical method of [9] with the top layer having elastic thickness $T_e = 0.4d$ and the underlying material having zero rigidity, appropriate to the case of a subsurface ocean. This method gives a range β = 1.7–1.2 for d = 2–10 km. Dotted curve assumes $\Delta\rho$ = 30 kg m^{-3} and calculates variable β using [9] assuming that the material beneath the rigid ice has rigidity 100 GPa, appropriate to a silicate core.

Fig. 2 demonstrates that significant poleward reorientation (up to 35^o) can occur for sufficiently large density contrasts (100 kg m^{-3}), if the lithospheric thickness exceeds ~2 km (thus T_e > ~1 km), and if the ice shell is decoupled from the silicate interior. Thus, the polar location of the hot-spot on Enceladus suggests that the satellite has managed to maintain some near-surface rigidity, despite the observed surface deformation. A temperature contrast of ~100 K will give rise to density contrasts of only ~10 kg m^{-3}. Because large density contrasts are required to achieve significant reorientation, the presumed diapir is likely to be primarily compositional, rather than thermal, in origin. For instance, partial melting of a tidally-heated diapir will preferentially remove low-melting temperature, dense components, such as salts, leading to compositional buoyancy [14,15]. For compositional (Rayleigh-Taylor) instabilities, the initial size of the diapir is usually comparable to the thickness of the fluid layer, which for a ~100 km thick Enceladus's ice mantle generates a feature of roughly the correct dimension. Larger density contrasts may arise due to diapiric activity within the silicate core [12], but the resulting reorientation is likely to be much smaller, owing to the factor $(R_C / R)^3 \approx 0.2$ in eqn (2). Moreover, core diapiric activity would require extreme internal heating.

Discussion and Summary: It is probably not a coincidence that the warm, active area of Enceladus is centered on the satellite's spin axis, as reorientation can be a natural consequence of the rise of a relatively large, low-density plume within the ice mantle of a small icy satellite. Interior processes can lead to the formation of single plumes, especially if large viscosity contrasts or compositional layering are involved [16]. Multiple, successive diapir and reorientation events may be possible, and might account for the somewhat older tectonically deformed regions of Enceladus. A warm low-viscosity ice mantle and an interior ocean will greatly facilitate reorientation by reducing the frozen-in tidal bulge of the shell; an ocean further decouples the shell from the interior, which may not reorient.

Reorientation may be a common feature of warm satellites that have large internal density variations, favoring reorientation of small but active icy satellites, specifically Enceladus and Miranda [17-19], which have thick ice shells relative to their radii. On the other hand, a small icy satellite that has not reoriented must be relatively rigid, as is likely true of Saturn's Mimas.

This hypothesis provides several testable predictions. First, we have provided a lower bound on the elastic thickness of the icy lithosphere of Enceladus, which may be determined independently if local topographic measurements become available. Second, true polar wander is expected to generate global tectonic stresses, leading to compression near the satellite poles and strike-slip or extensional activity nearer the equator [20]. These stress patterns, however, are likely to be complicated by other sources of global stress, such as diurnal tides, non-synchronous rotation, or ice shell thickening, in addition to the deformation generated by the rising diapir itself [cf. 17]. Third, the distribution of impact craters [18], expected to show leading-trailing asymmetry, is expected to be affected by—and could constrain—the history of reorientation.

References: [1] Spencer, J.R., et al., *Science*, in press. [2] Porco, C.C., et al., *Science*, in press. [3] Ojakangas, G. W. and D. J. Stevenson, *Icarus*, *81*, 242, 1989. [4] Willemann, R. J., *Icarus*, *60*, 701, 1984. [5] Matsuyama, I., et al., *JGR*, in press. [6] Greenberg, R., and S. T. Weidenschilling, *Icarus*, *58*, 186, 1984. [7] Tsai, V.C. and D.J. Stevenson, *JGR*, submitted. [8] Ross, M.N. and G. Schubert, *Icarus*, *78*, 90, 1989. [9] Harrison, J.C., *JGR*, *68*, 4269, 1963. [10] Moore, W.B. and G. Schubert, *Icarus*, *147*, 317, 2000. [11] Turcotte, D. et al., *JGR*, *86*, 3951, 1981. [12] Matson, D.L. et al., *Eos*, *86(52)*, P32A-03, 2005. [13] Nimmo, F., et al., *GRL*, *29(7)*, 10.1029/2001GL013976, 2002. [14] Nimmo, F., et al., *Icarus*, *166*, 21, 2003. [15] Pappalardo, R. T. and A. C. Barr, *GRL*, *31*, 10.1029/2003GL019202, 2004. [16] Roberts, J.H. and S. Zhong, *JGR*, submitted. [17] Janes, D.M., and H.J. Melosh, *JGR*, *93*, 3127, 1988. [18] Plescia, J.B., *Icarus*, *73*, 442, 1988. [19] Pappalardo, R.T., et al., *Eos*, *86(52)*, P22A-06, 2005. [20] Melosh, H.J., *Icarus*, *43*, 334, 1980.